State of Charge Prediction Framework for Lithium-Ion Batteries Incorporating Long Short-Term Memory Network and Transfer Learning

Yu Liu[1], Xing Shu[2**], Hanzhengnan Yu[1], Jiangwei Shen[2], Yuanjian Zhang[3], Yonggang Liu[4], Zheng Chen[2,5*]
[1]China Automotive Technology and Research Center Co., Ltd., Tianjin, 300300, China.
[2]Faculty of Transportation Engineering, Kunming University of Science and Technology, Kunming, 650500, China.
[3]School of Mechanical and Aerospace Engineering, Queen's University of Belfast, BT9 5AG, Northern Ireland.
[4]State Key Laboratory of Mechanical Transmissions & School of Automotive Engineering, Chongqing University, Chongqing, 400044, China
[5]School of Engineering and Materials Science, Queen Mary University of London, London, E1 4NS, United Kingdom.
Email: liuyu2016@catarc.ac.cn, y.zhang@qub.ac.uk, yuhanzhengnan@catarc.ac.cn, andylyg@umich.edu, chen@kust.edu.cn
Corresponding Authors: Zheng Chen (chen@kust.edu.cn) and Xing Shu (shuxing92@kust.edu.cn)

Abstract: This study investigates accurate state of charge estimation algorithms for lithium-ion batteries based on the long short-term memory recurrent neural network and transfer learning. The long short-term memory network with the five typical layer topology is firstly constructed to learn the dependency of state of charge on measured variables. The transfer learning algorithm with fine-tuning strategy is then exploited to regulate the parameters of fully connected layer and share the knowledge of other layers. By this manner, the information from the source data can be applied to predict state of charge of other batteries with less training data. Additionally, a rolling learning method is developed to update the model parameters when the battery capacity is degraded. The precision and robustness of the proposed framework are comprehensively validated through comparative analysis of multitudinous sets of hyperparameters and methods. The experimental results manifest that the developed framework highlights precise estimation capability of state of charge at different aging states and time-varying temperature conditions. In addition, the proposed algorithm is verified feasible when transferred to different batteries based on only 30% training data.

Key Words: Lithium-ion battery, long short-term memory network, state of charge, temperature variation, transfer learning.

I. INTRODUCTION

As a promising electrical energy storage media, lithium-ion batteries have been extensively assembled in electric vehicles (EVs) and power grid, due to their wide temperature range, high power density and low memory effect [1]. To ensure working safety and prolong service life, battery management system (BMS) is usually indispensable for monitoring and controlling their proper and safe operation [2]. State of charge (SOC), as one crucial parameter inside of batteries, indicates the percentage of remaining capacity over the nominal value [3]. Accurate and reliable SOC can not only provide useful information on how much capacity is left in the battery or how long the battery can be fully charged, but also supply the guidance for avoidance of over charge/discharge [4]. However, it can not be measured directly by existing external electrical sensors but can be indirectly estimated based on the measurements. As such, a variety of efforts have been devoted to designing efficient, accurate, and robust SOC estimation algorithms [5]. To now, these methods can be simply classified into four categories: ampere-hour (Ah) integration method, open circuit voltage (OCV)-based method, data driven-based methods and filter-based methods [6].

The Ah integration method calculates SOC by integrating the current flowing through batteries with a known initial SOC value [7]. It is simple and widely implemented in practice [8]. Yet, it is difficult to pledge the estimation precision, as it is sensitive to current measure noise and initial value of SOC. The OCV-based method leverages the correlation between OCV and SOC to forecast SOC [9]. Apparently, it can not be employed for real applications as the OCV can only be acquired by shelving the battery for a sufficiently long time, usually more than two hours [10]. Additionally, when the battery OCV varies slowly with SOC, especially when the voltage locates in a plateau area, tiny OCV derivation may lead to large SOC estimation error. By merging the OCV-based method and Ah integration method, the filter-based methods are proposed and applied to estimate SOC with the support of offline built electric models [11]. Obviously, the electric model and filter algorithm are two essential elements for SOC estimation. For the former one, equivalent circuit models (ECMs) [12], complex electrochemical models [13] and machine learning models (particularly neural networks (NNs)) [14] have been widely investigated to characterize electrical performances of batteries together with advanced parameter estimation algorithms, such as recursive least square (RLS) [15] and genetic algorithm (GA) [16]. For the latter item, the most widely used algorithm is Kalman filter

(KF) and its extended form, referred to as extended KF (EKF), which conducts partial derivatives to linearize the battery nonlinear voltage variation in terms of SOC [17]. In [18], a feedforward NN (FF-NN) is introduced to depict the polarization characteristics of batteries, and then the EKF is employed to estimate SOC. In addition to EKF, other filtering methods, including unscented KF (UKF) [19], cubature KF (CKF) [20], particle filter (PF) [21] and H-infinity filter (HIF) [22], are also commonly preferred for SOC prediction. These methods are effective in eliminating the initial SOC difference and noise interference [23]. However, they are difficult to cope with temperature variation and capacity degradation, even massive efforts have been made to mitigate these passive influences.

To overcome this drawback, black box models fully taking advantage of data driven methods are introduced for SOC estimation. With the development of data storage technologies and the improvement of computing capacity furnished by graphics-processing units (GPU), data driven-based methods have progressively drawn much attention from the research and application perspectives [24]. Data driven based methods can reveal the latent SOC relationship with the measured variables and historical operation information. These methods only need to excavate the nonlinear relationship between input variable and output data, and do not need to account for interior complex electro-chemical reactions of batteries [25]. Ref. [26] designs a recurrent NN (RNN) with the gated recurrent units to predict battery SOC based on the measured temperature, voltage and current. To tackle the aging influence, Ref. [27] employs the RNN to simultaneously predict SOC and state of health (SOH), and verifies the feasibility of the developed approach on different types of lithium-ion batteries. Due to the gradient vanishing problem of RNN during back-propagation training processes, the long-term dependency is difficult to be captured. In this context, long short-term memory (LSTM), as an evolution of conventional RNN, has been widely applied in state prediction with the capacity of tackling time-series information [28]. Ref. [29] exploits the LSTM network to estimate SOC and showcases the ability of encoding dependencies in time without any dependence on battery models. In [30], a mixed convolutional NN (CNN)-LSTM network is constructed to map the nonlinear dynamic relationship between SOC and voltage, current and temperature. In [31], an autoencoder NN is proposed for feature extraction, and the results of the hidden layer in the NN is taken as the inputs of LSTM for SOC estimation.

Although a large number of data-driven approaches have successfully emerged to estimate SOC, existing approaches still have some obvious drawbacks. Firstly, the temperature influence on SOC estimation is not sufficiently taken into consideration. Most of the existing methods are usually validated only at a fixed temperature or limited temperature range. However, the working environment of battery is execrable, and the ambient temperature is usually time-varying, therefore the proposed method should be capable of adapting continuous variation of temperature. Secondly, the cycling operation of batteries leads to capacity degradation, and traditional methods assume that the capacity is known beforehand; and additionally, joint estimation methods are usually devised to simultaneously estimate the SOC and capacity/SOH. However, more estimation tasks will no doubt complicate the estimation algorithm design, and correspondingly increase the computational intensity. Thirdly, conventional data driven approaches employ statistical models to forecast future behavior, and these models are trained based on the offline measured data, which entail elaborate experiments with the full consideration of different operation circumstances. If the previous learning knowledge on one battery can be transferred to new batteries or even new types of batteries, the interactable computation burden when constructing new battery models can be significantly mitigated, and therefore the advantages of data driven methods can be further promoted. Fortunately, transfer learning (TL) can refer to the knowledge from one domain and extend it to another domain with the same or similar properties. It may contribute to data driven based SOC estimation with less computation burden and training data preparation [32].

To overcome the discussed bottlenecks when employing data driven methods to estimate SOC, an effective SOC estimation framework incorporating the LSTM network and TL is, to the authors' knowledge, firstly proposed in this study. The LSTM model with five layers is developed to predict SOC based on the well-prepared data of source battery. To tackle the variation of temperature and degradation, the TL with fine-tuning strategy is introduced to modify partial model parameters. Furthermore, a rolling learning method is developed to update the model parameters especially when the battery capacity is degraded. Compared to conventional filter based methods and support vector machine (SVM) method, the proposed framework can well adapt to the rapid variation of ambient temperature and capacity degradation, and meanwhile highlight satisfactory SOC estimation accuracy. In addition, the computation burden can be dramatically lessened when conducting new battery SOC estimation, due to the simplified model training job incurred by TL.

The remainder of this study is structured into four parts: Section II preliminarily introduces the whole estimation framework and the theoretical basis of LSTM and TL. Section III elaborates the procedure for SOC prediction. The experimental validation and discussion are given in Section IV. The main conclusions of this study are presented in Section V.

II. METHODOLOGY

The target of this study is to find hidden variation laws between SOC and measure variables. To attain robust design, a LSTM model incorporating TL is proposed, as shown in Fig. 1. The LSTM network is established to map the nonlinear relationship between SOC and current, voltage and temperature. Meanwhile, to improve the environmental adaptivity and reduce the number of training sets, TL is harnessed to adjust the model parameters of LSTM. In this section, these two key components of the framework will be introduced in detail.

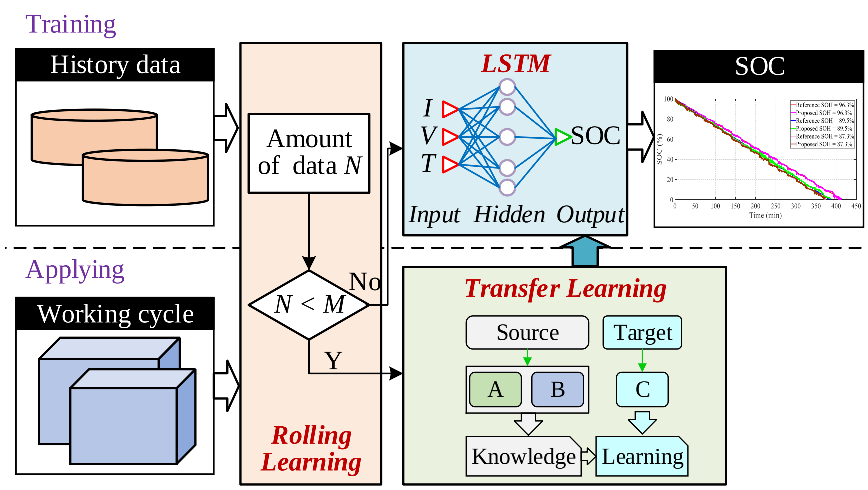

Fig. 1. Construction of the proposed framework.

A. Long Short-Term Memory Network

LSTM network belongs to a special class of RNN. For traditional RNNs, there exists only one hyperbolic tangent layer in the recurrent modules. Nevertheless, the knowledge from foregoing steps generates only neglectable impression on the current output, as shown in Fig. 2 (a), where darker circles symbolize more sensitive degree. As an improved model of RNNs, LSTM features the similar sequence or chain configuration, however, the LSTM module shows a different structure. In contrast to standard RNN, there exist five layers that are related to each other in a special topology. Fig. 2 (b) details the main topology of LSTM, which mainly includes three units, i.e., input, output and forget gates, to remember long-term information; and these gates are merged together to determine which information will be memorized or forgotten. Usually, the *tanh* function and *sigmoid* function are executed to select the information.

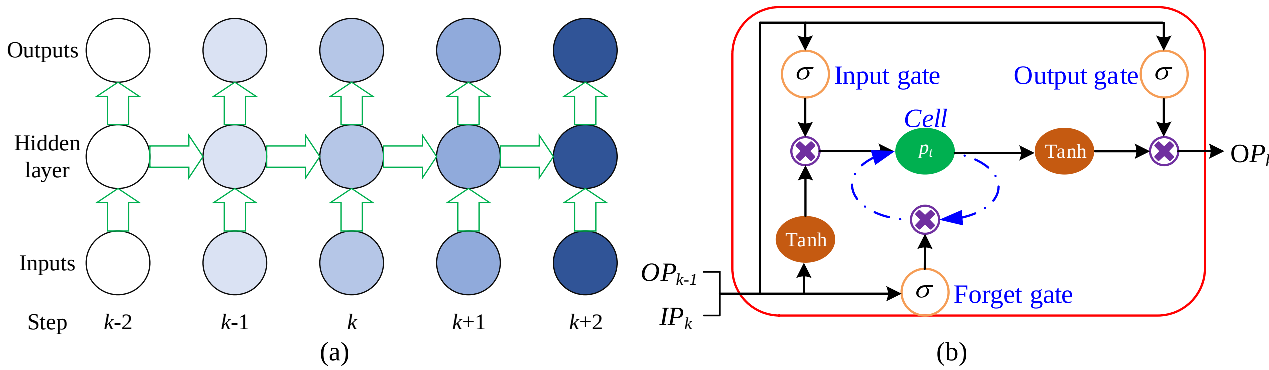

Fig. 2. Structure of RNN and LSTM: (a) Standard RNN; (b) LSTM.

The priority work of implementing LSTM is to determine what messages are going to be neglected by the forget gate. It squashes the inputs of IP_k and OP_{k-1} into 0 to 1, where IP_k denotes the input of current step, OP_{k-1} means the output of step $k-1$, the upper value 1 means the value should be retained totally; and on the contrary, the lower boundary 0 indicates discarding the information completely. The forget gate can be expressed as [14]:

$$f_k = \sigma(b_f + IP_k IW_f + OP_{k-1} OW_f) \tag{1}$$

where f, i, O and c respectively represent the forget, input, output gates and memory cell, $b_\cdot$ indicates the bias of forget gate, $OW_\cdot$ and $IW_\cdot$ correspondingly denote the weights for last output and input. Then, what message should be stockpiled needs to be judged. This step includes two parts: the first part, called “input gate”, adjudicates which value needs to be updated; and the second part, called “input node”, creates a new candidate vector, as:

$$\begin{cases} i_k = \sigma(b_i + IP_k IW_i + OP_{k-1} OW_i) \\ g_k = \tanh(b_g + IP_k IW_g + OP_{k-1} OW_g) \end{cases} \tag{2}$$

Correspondingly, the current cell state can be calculated as:

$$c_k = c_{k-1} f_k + g_k i_k \tag{3}$$

Eventually, the output gate determines what information will be outputted with the help of the updated cell state, the information of input gate and input node, as:

$$\begin{cases} O = \sigma(b_O + IP_k IW_O + OP_{k-1} OW_O) \\ OP_k = \tanh(p_k) \cdot O \end{cases} \tag{4}$$

where p_k denotes the internal variable of LSTM cells.

B. Transfer Learning

The learning processes for traditional LSTM and LSTM with TL (called LSTM-TL hereinafter) are elucidated in Fig. 3. As can be seen, conventional LSTM handles each task from different data sources, while TL borrows the information from a formerly learned source task for training the target task, and can effectively avert "training from scratch". In TL, the existing knowledge is called source domain, and the new knowledge to be learned is defined as target domain. In particular, TL studies how to apply existing models to a novel and different but related field. Traditional LSTM is not flexible enough when dealing with the tasks of data distribution, dimension and model output change, while TL does not require the training set and test set to be with the same distribution. Under the condition of acquiring data distribution, feature dimension and model output variation, the knowledge in source domain can be exploited to better model the target domain. In addition, in the case of lacking enough calibration data, TL can make full use of the calibrated data in other related fields to compensate the data shortage. In this study, it is assumed that the features and data distribution of different lithium-ion batteries are various but correlated. By this manner, LSTM in combination with TL can be hired to estimate SOC for different batteries, and the detailed implementation process will be elaborated in the following section.

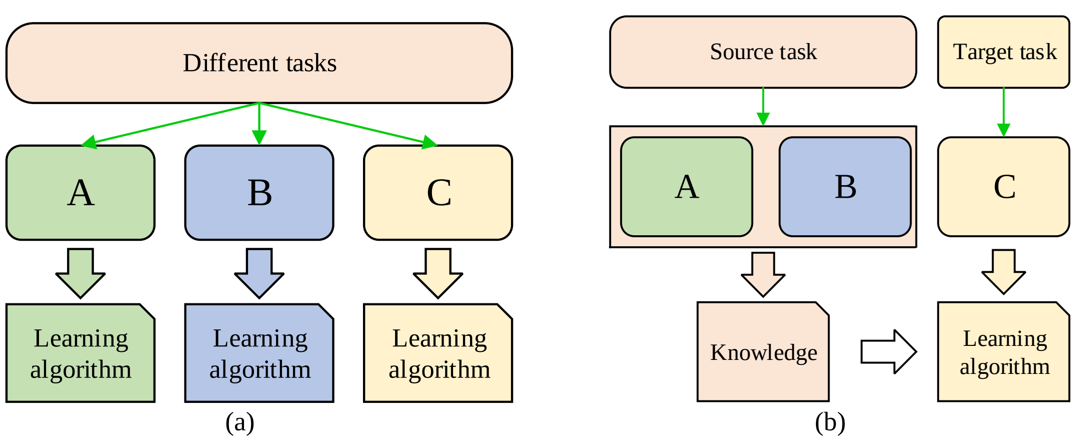

Fig. 3. Learning process for different learning methods: (a) Conventional learning process; (b) Transfer learning process.

III. State of Charge Estimation Based on Improved LSTM and TL

The overall framework of the proposed SOC estimation, as detailed in Fig. 4, is roughly divided into two parts: 1) the source and target network training and SOC estimation; and 2) rolling learning [33].

The LSTM method is manipulated to establish a source LSTM network for SOC estimation of battery A (here A and B represent different types of batteries) according to the measurement. It is well known that the selection of battery measurement signals for network inputs is not an easy task; however, current, temperature and voltage are the directly measured parameters, and they have also been verified critical to aid internal state estimation of batteries [34]. These three parameters are extracted as the sequence input features of LSTM in this study. It should be noted that when the internal temperature of battery changes, the measured temperature will also vary, and the activation characteristics of lithium ions in the battery will change simultaneously, leading to the voltage profile variation. Therefore, when the voltage and temperature are taken as the input of LSTM, the influence of temperature on SOC is indirectly considered. Additionally, the structure of LSTM for regression consists of five layers, i.e., input layer, LSTM layer, dropout layer, fully connected layer and regression output layer.

After obtaining the parameters of LSTM network, the parameters will be transferred to the target LSTM network which is trained in terms of different types of healthy and aged batteries. In this study, the fully connected layer would be retrained to learn the diversities between the source battery and target battery, and the parameters of other layers remain the same. In the retraining process, only 30% data are harnessed for model training, and the rest 70% data will be applied for estimation performance validation.

A common knowledge is that battery aging imposes significant influence on SOC estimation, and it is intractable to accurately estimate SOC of the aged battery without considering capacity degradation. During training, the collected operation data are classified into input features and output dataset, by which the model can map the affine relationships between features and SOC. Inspired by model predictive control (MPC), a rolling learning method is proposed to update the model parameters of LSTM for tackling the aging influence on SOC. The rolling learning algorithm consists of three parts: data accumulation, feedback correction and rolling optimization. As shown in Fig. 4, when the battery management unit works, the battery operation data will be continuously collected. After a period of time, if the amount of accumulation data N is more than the preset length M. Then, the LSTM network will be retrained and calibrated by the TL, and a group of new parameters of LSTM will be exploited to predict SOC. By means of the rolling-learning mechanism, LSTM enables to take the historical influence into account, so as to conduct expected estimation by the propose LSTM-TL cooperation framework. Moreover, the inputs of the proposed method include current, voltage and temperature, and it is not necessary to know the battery capacity value. By this manner, the difficulty of capacity or SOH estimation can be effectively mitigated.

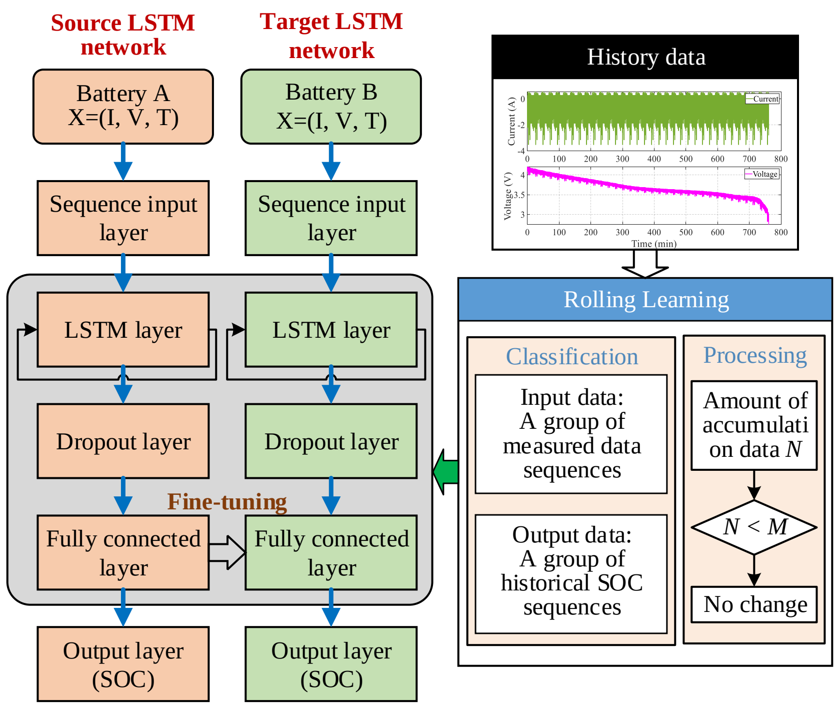

Fig. 4. Flowchart of the SOC estimation framework.

The whole operation procedure can be described as follows. Firstly, the historical data are collected and stored by system and inputted into the feedback corrector. Then, for achieving high-precision optimal control, enhancing the anti-interference ability of system and improving the control stability, the feedback correction is furnished to amend the control parameters of LSTM according to the historical data. Given the corrected parameters of LSTM at the current step, the state value in the subsequent time domain is estimated by the newly updated model parameters until the next receding horizon is reached. The above steps will be repeated until the termination of estimation.

In the following section, experimental validations and discussions will be conducted to validate the feasibility of the proposed framework.

IV. EXPERIMENTAL VALIDATION AND DISCUSSION

A series of validations are carried out in this paper to verify the proposed estimation framework. Firstly, the number of units for the source LSTM is determined. Secondly, the estimation results at different ambient temperatures are presented and compared with traditional algorithms, including SVM and AEKF. Thirdly, the expansibility of the presented framework is discussed based on different types of batteries. Finally, the adaptability and robustness of the proposed method are justified at different aged cells. All the simulations presented in this study are performed on a desktop computer equipped with Intel Xeon E3-1230 (3.30 GHz) processor and 32 GB memory. To fully evaluate the performance of the presented method, three evaluation criteria are indexed, including average absolute error (AAE), maximum absolute error (MAE) and root-mean-square error (RMSE), as:

$$\begin{cases} AAE = \dfrac{1}{N_{sam}} \sum_{i=1}^{N_{sam}} \left| SOC_i - S\hat{O}C_i \right| \\ MAE = max \left| SOC_i - S\hat{O}C_i \right| \\ RMSE = \sqrt{\dfrac{1}{N_{sam}} \sum_{i=1}^{N} (SOC_i - S\hat{O}C_i)^2} \end{cases} \tag{5}$$

where SOC_i and $S\hat{O}C_i$ denote the reference value and estimation value at the *i*th sampling step, respectively; and N_{sam} means the total sampling number.

A. Parameter Selection

Before training the LSTM network, the model parameters need to be assigned. Actually, it is a challenging task to find the optimal parameters of LSTM, therefore the parameters need to be preset empirically, and then will be optimized through iterative optimization to attain better performance. Among all the parameters, the number of LSTM units influences the accuracy and complexity of the established model mostly. Thus, different numbers of hidden units are preferred to evaluate the model performance. In this case, the experiment is conducted at 30 ℃, and the nickel cobalt manganese (NCM) batteries are experimented in the case study of this paper. The fully charged battery is cycled under urban dynamometer driving schedule (UDDS), until its terminal voltage drops to its cut-off voltage of 2.75 V. The sampling frequency is set as 1 Hz.

Fig. 5 (a) and (b) demonstrate the SOC prediction results using different unit numbers of LSTM from 20 to 500 with an increase interval of 20. Fig. 5 (c) to (f) portray the performance metrics for different LSTM units. As can be found, there does not exist significant correlation between the estimation performance and the number of units. The best AAE, MAE, RMSE and running time appear in 340, 360, 340 and 20 units. From these results, it is difficult to choose the optimal unit. To tackle this problem, the entropy weight method is employed to score the prediction results, due to its strong capability in describing the disorder degree of information system [35]. Assuming that there exist a evaluation indexes and d evaluation objects in the original data, the performance value is normalized and limited to the range of [0, 1] for minimizing the difference between the data of each dimension of the evaluation index, as:

$$P_{q,p} = \frac{IV_{q,p} - min(IV_{\bullet,p})}{max(IV_{\bullet,p}) - min(IV_{\bullet,p})} \tag{6}$$

where $IV_{q,p}$ means the *p*th index value of the *q*th unit, $min(IV_{\bullet p})$ and $max(IV_{\bullet p})$ represent the minimum and maximum value of the *p*th index; thus $q \le a$ and $p \le d$. Then, the entropy of the *p*th index En_p can be formulated, as:

$$En_p = -(\log d)^{-1} \sum_{j=p}^{d} P_{q,p} \log P_{q,p} \tag{7}$$

The entropy weight of each index w_p can be calculated, as:

$$w_p = \frac{1 - En_p}{d - \sum_{p=1}^{d} En_p} \tag{8}$$

Thus, the score $Score_p$ can be calculated as:

$$Score_p = P_{q,p} {w_p}^T \tag{9}$$

The scoring results are displayed in Fig. 5 (g). It can be observed that the LSTM network with 120 units leads to the highest score 0.92, while the model with 20 units shows the lowest value 0.3. That is, the LSTM model with 120 units can achieve a preferable trade-off between the estimation precision of SOC and the running time. As such, 120 hidden units are selected for LSTM construction and SOC prediction.

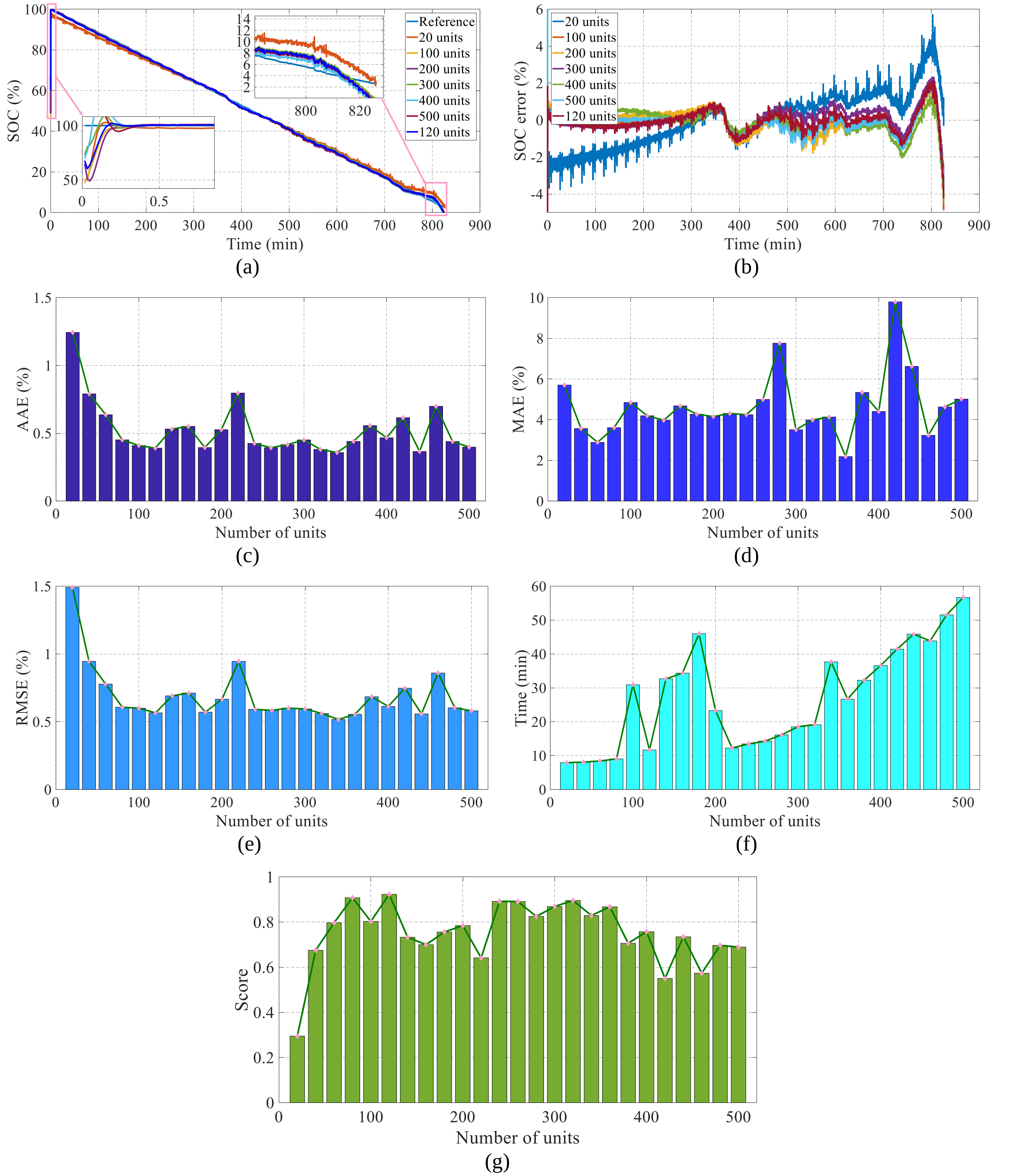

Fig. 5. SOC Estimation results using different numbers of hidden units: (a) Comparison of SOC; (b) SOC estimation errors; (c) AAE; (d) MAE; (e) RMSE; (f) Running time; (g) Scores of different numbers of units.

B. Evaluation Results at Varying Ambient Temperatures

It is well acknowledged that battery capacity and power highly depend on temperature; as such, the qualified SOC estimation should be capable of well adapting to ambient temperature variation. To validate it, the battery is experimented with the dynamic current profiles under time-varying temperatures conditions ranging from 15 to

55 ℃. The temperature is first set to 55 ℃ for one hour and then is reduced by 5 ℃. Next, the battery is maintained at the temperature for another one hour. Repeat the above process until the end of discharge. During the test, the federal urban driving schedule (FUDS) current profile is imposed to discharge the battery until 2 Ah capacity is released, followed by constant current-constant voltage (CC-CV) charge (CC: 0.5C current and CV: 4.2 V). Finally, the FUDS cycle test is performed again until the voltage drops to 2.75 V. Fig. 6 (a) delineates the current and voltage responses, and Fig. 6 (b) shows the temperature variation. In addition, to evaluate the performance of the developed framework based on LSTM and TL, we compare it with the SVM estimation algorithm, which adopts the same data for modeling training, and with the AEKF estimation based on the first-order ECM. The inputs of the proposed method and SVM are battery terminal voltage, current and temperature; and for SVM and the proposed method, it is not necessary to know the initial SOC in advance. While when applying the AEKF for SOC estimation, an initial SOC is necessary for model input. From this point of view, an initial SOC error is only set in AEKF, which is set to 60% with initial error of 40%. For fairly examining the convergence performance of the proposed method, the initial inputs of the proposed method and SVM including current, voltage and temperature are mistakenly set to 2 A, 2.75 V and 25 ℃, respectively, in contrast to the real initial values of -0.01 A, 4.19 V and 49.72 ℃.

The estimation results of these methods are depicted in Fig. 6 (c) and (d) and tabulated in Table I. As can be found, the SOC by the proposed method can follow the reference value during the whole discharge and charge processes, with the overall error of less than 4%, while it is difficult for AEKF to compensate the influence of temperature on SOC estimation, enabling the error to increase gradually with temperature variation. Nonetheless, the estimation error of these three methods is significantly reduced in the CC-CV charging stage, and the estimation curve becomes smoother. As listed in Table I, the AAE obtained by these three methods is 3.27%, 0.94% and 0.53%, respectively; and the MAE by the proposed method is 3.80%. For AEKF and SVM, the MAE is 5.8% and 16.10%, obviously higher than that of the developed algorithm. The RMSE of AEKF and SVM algorithm is five and two times than that of the proposed framework. Additionally, the duration to reach the reference SOC value for AEKF, SVM and the proposed method is respectively 216 s, 2 s and 30 s. Although the convergence time of SVM is less than that of the proposed method, the estimation results by the SVM fluctuate obviously in the low SOC stage. Hence, it can be concluded that the proposed method outperforms the other two algorithms in both convergence performance and stability, and the proposed framework is more suitable for SOC estimation and leads to higher estimation accuracy.

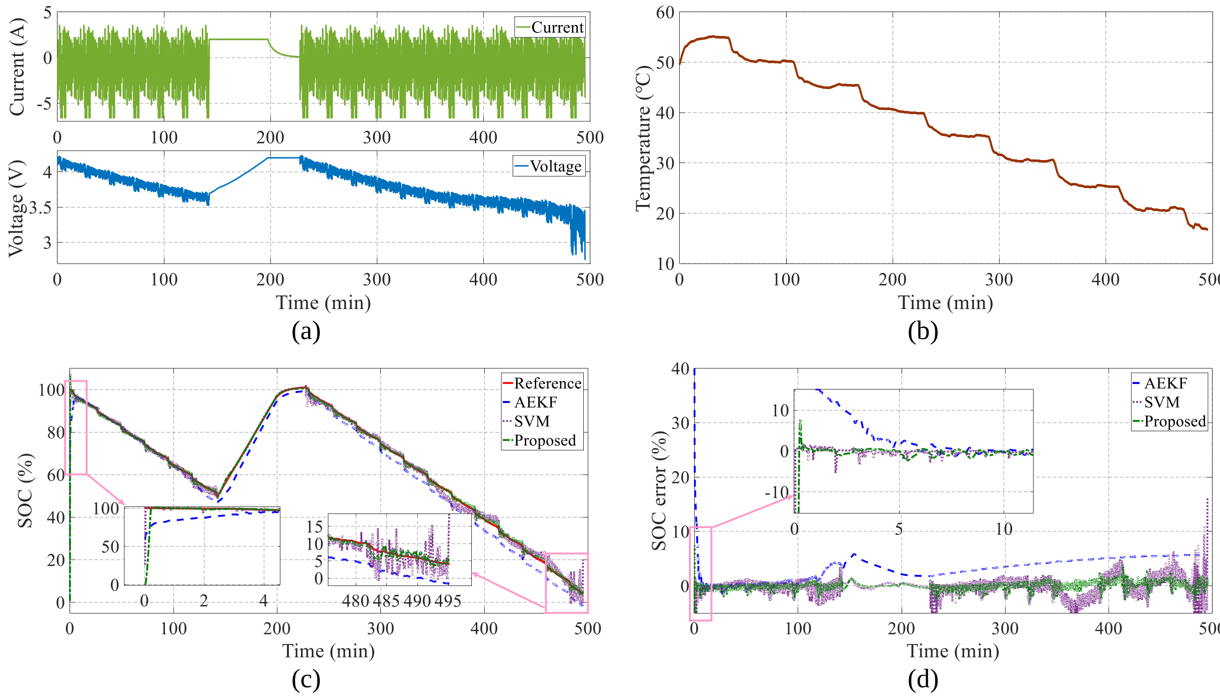

Fig. 6. SOC evolution curves at varying ambient temperatures and different methods: (a) Current and voltage response curves; (b) Ambient temperature change curve; (c) SOC evolution curves; (d) Estimation errors.

Table I. Comparison of SOC Estimation for Different Methods

Method	Convergence time (s)	AAE (%)	MAE (%)	RMSE (%)
AEKF	216	3.27	5.80	3.90
SVM	2	0.94	16.1	1.38
Proposed	18	0.53	3.80	0.69

C. Evaluation Results at Different Batteries

To validate the transfer ability of the proposed framework, the well-trained network is extended to implement in another type of lithium-ion batteries, i.e., lithium cobalt oxide (LCO) battery, of which the data comes from the Center for Advanced Life Cycle Engineering [36]. The battery is discharged at 25 ℃ with US06 cycle, and the specific implementation process can be found in [36]. The experimental results are sketched in Fig. 7, where “LSTM” indicates the estimation results by single LSTM method using 70% training data, and “Proposed” represents the prediction results by LSTM combining TL using 30% training data. It can be seen that the LSTM and the presented framework feature similar prediction performance. The MAE of these methods are all lower than 5%. The running time of each method per step is also calculated. Concretely, the running time per step of the LSTM and the proposed method is 0.023 s and 0.0077 s, respectively. Obviously, the proposed framework is more efficient than that of single LSTM method without error increase. Moreover, compared with the training data amount for the single LSTM method, the training data size for the proposed framework can be reduced by 40%, while the prediction performance is not deteriorated. As such, it can be concluded that the proposed algorithm can be transplanted from NCM batteries to LCO batteries with easy extendibility. The only task that needs to be conducted is to adjust the parameters of one middle layer. By this manner, the accuracy and feasibility of the proposed framework is verified when applying in different types of batteries.

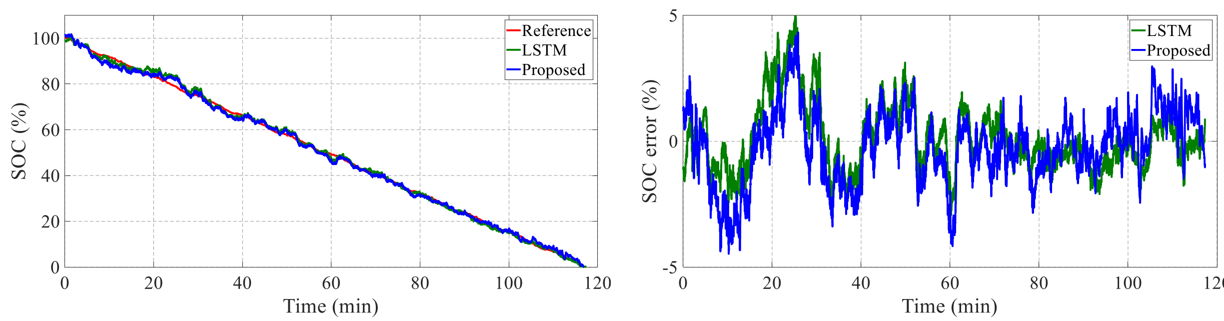

(a) (b)

Fig. 7. SOC evolution curves at different batteries: (a) SOC evolution curves; (b) Estimation errors.

D. Evaluation Results at Aging Batteries

According to the proposed rolling learning method, the battery cells cycled at different aging states are tested to verify the adaptivity of the proposed SOC estimation framework. Here, three different aged cells, whose SOH is respectively 96.3%, 89.5% and 87.3%, are cycled with the FUDS and UDDS current at 25 °C. The SOC prediction and statistic results are demonstrated in Fig. 8 and Table II, respectively.

Fig. 8 (a) to (c) show the corresponding current and voltage profiles. As can be seen, cells 1 and 3 are with the same discharge cycles, and both are circularly discharged with the hybrid FUDS and UDDS cycle. While cell 2 is firstly discharged by the FUDS, followed by the CC-CV charge. Then, it is discharged under the repetitive UDDS experiment. For cells 1 and 3, the current in the first discharge cycle is larger than that in the second cycle. By contrast, the current of cell 2 in the first discharge stage is smaller than that in the second stage. The data of the first cycle are chosen as the training dataset, and the data of the second cycle are considered as the test dataset. By this manner, the dynamic current profiles can well verify the generalization ability of the proposed method.

Fig. 8 (d) and (e) depict the SOC variation and error, respectively. Fig. 8 (d) highlights that the proposed method can precisely predict SOC, even when the battery is aged with different states. Moreover, although the aging level and discharge current of these three batteries are different, their SOC error appears more consistently. During the intermediate stage of the discharging process (e.g., 30% to 60%), the estimation error slightly increases, owing to the discounted network model accuracy incurred by the plateau characteristic of voltage responses. Even so, they can all converge to a satisfied level. All the MAE of the proposed method for three cells can be maintained within 3%, as described in Fig. 8 (d). Table II lists the AAE, MAE and RMSE of the SOC prediction results based on the proposed framework. The corresponding AAE and RMSE values of the proposed method for different aging states are also similar, and these boundary can be maintained within 0.3% and 0.6%, respectively. To sum up, the designed LSTM-TL, together with the rolling learning method, can not only be employed to authentically forecast the SOC, but also furnish higher robustness when the battery capacity is degraded.

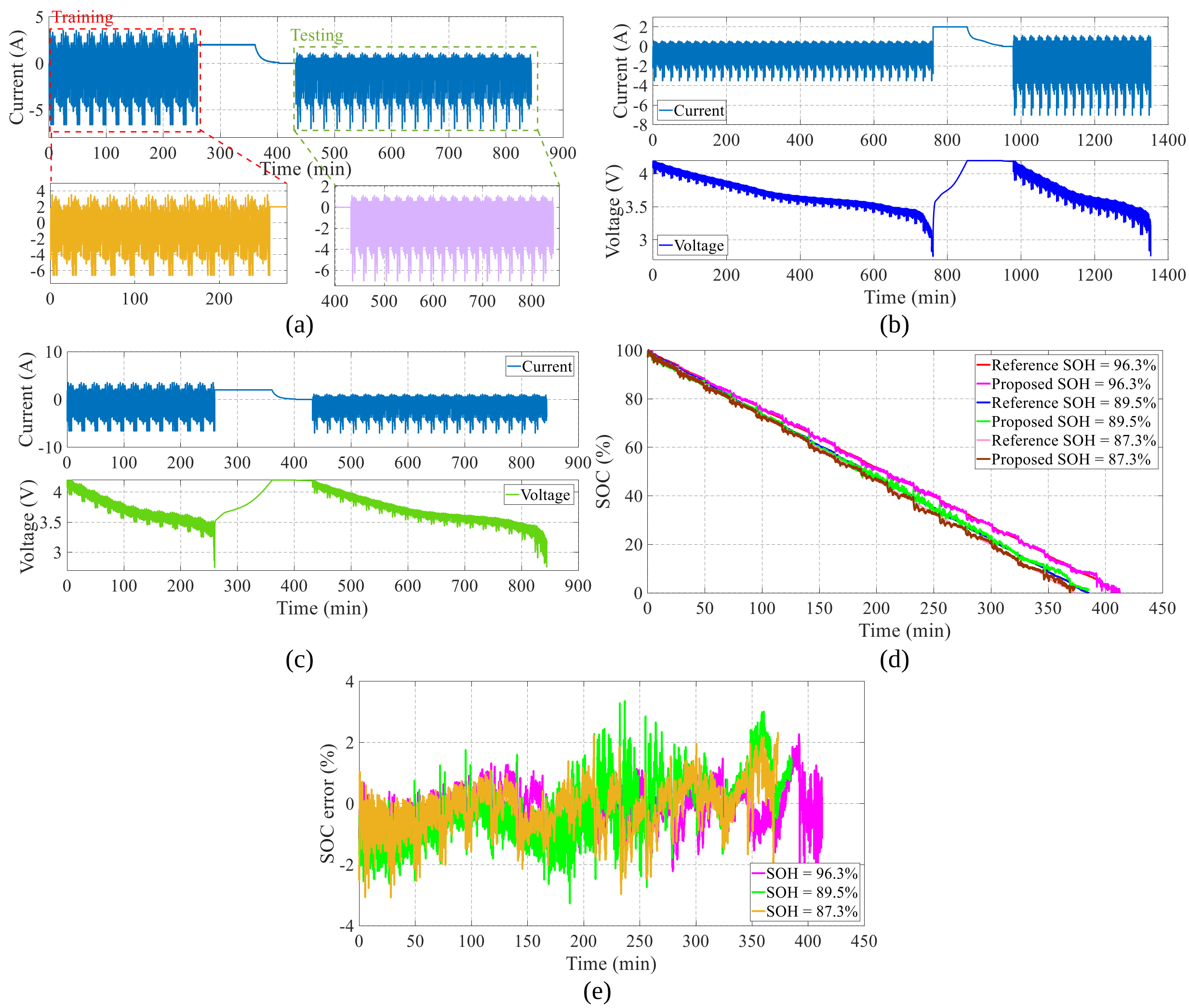

Fig. 8. Evaluation results at aging batteries: (a) Training and testing datasets for aging cell 1; (b) Current and voltage profiles for cell 2; (c) Current and voltage profiles for cell 3; (d) SOC evolution curves; (e) Estimation errors.

Table II. Comparison of SOC Estimation for Aging Batteries

SOH	AAE (%)	MAE (%)	RMSE (%)
96.3%	0.26	2.98	0.45
89.5%	0.24	3.3	0.55
87.3%	0.18	3.08	0.43

V. CONCLUSIONS

Data driven estimation methods have been authenticated to be effective in state of charge estimation. However, they are impeded by vast demand of training data. To cope with this restriction, this study combines the long short-term memory network with transfer learning and rolling learning algorithms to conduct state of charge prediction. Given the five layer topology, the long short-term memory network is constructed to catch the nonlinear characteristics of state of charge based on current, voltage and temperature without any pre-processing. The developed long short-term memory transfer learning framework allows the long short-term memory network to fully account for the environmental temperature influence. By applying the transfer learning with fine-tuning strategy, the well-trained long short-term memory network based on the source battery can be transferred to the target battery based on only 30% data, observably improving the practicability and efficiency in state of charge prediction. The model training speed by the transfer learning is much faster than that of the re-training process. Moreover, a rolling learning method is proposed to improve the algorithm robustness when the battery is degraded. The experimental validation reveals that the proposed framework can conduct precise state of charge estimation with the error of less than 4%. The comparative experimental validations justify the framework's feasibility, robustness and adaptivity in state of charge estimation.

In the future, more sets of history data will be integrated into the long short-term memory model, especially under time-varying working conditions. How to improve the self-learning ability of long short-term memory for better state estimation of lithium-ion batteries is also our research direction.

ACKNOWLEDGEMENTS

This work was supported in part by the National Key R&D Program of China (No. 2019YFC1907901), in part by the National Natural Science Foundation of China (No. 61763021), and in part by EU-funded Marie Skłodowska-Curie Individual Fellowships Project under Grant 845102-HOEMEV-H2020-MSCA-IF-2018.

REFERENCES

[1] Y. Wang and Z. Chen, "A framework for state-of-charge and remaining discharge time prediction using unscented particle filter," *Applied Energy,* vol. 260, p. 114324, 2020.

[2] X. Shu, G. Li, Y. Zhang, J. Shen, Z. Chen, and Y. Liu, "Online diagnosis of state of health for lithium-ion batteries based on short-term charging profiles," *Journal of Power Sources,* vol. 471, p. 228478, 2020.

[3] X. Shu, G. Li, J. Shen, Z. Lei, Z. Chen, and Y. Liu, "An adaptive multi-state estimation algorithm for lithium-ion batteries incorporating temperature compensation," *Energy,* vol. 207, p. 118262, 2020.

[4] Y. Wang, J. Tian, Z. Sun, L. Wang, R. Xu, M. Li, and Z. Chen, "A comprehensive review of battery modeling and state estimation approaches for advanced battery management systems," *Renewable and Sustainable Energy Reviews,* vol. 131, p. 110015, 2020.

[5] M.-F. Ng, J. Zhao, Q. Yan, G. J. Conduit, and Z. W. Seh, "Predicting the state of charge and health of batteries using data-driven machine learning," *Nature Machine Intelligence,* pp. 1-10, 2020.

[6] R. Xiong, J. Cao, Q. Yu, H. He, and F. Sun, "Critical review on the battery state of charge estimation methods for electric vehicles," *Ieee Access,* vol. 6, pp. 1832-1843, 2017.

[7] S. Boulmrharj, R. Ouladsine, Y. NaitMalek, M. Bakhouya, K. Zine-dine, M. Khaidar, and M. Siniti, "Online battery state-of-charge estimation methods in micro-grid systems," *Journal of Energy Storage,* vol. 30, p. 101518, 2020/08/01/ 2020, doi: https://doi.org/10.1016/j.est.2020.101518.

[8] L. Hu, X. Hu, Y. Che, F. Feng, X. Lin, and Z. Zhang, "Reliable state of charge estimation of battery packs using fuzzy adaptive federated filtering," *Applied Energy,* vol. 262, p. 114569, 2020.

[9] Z. Wei, G. Dong, X. Zhang, J. Pou, Z. Quan, and H. He, "Noise-immune model identification and state of charge estimation for lithium-ion battery using bilinear parameterization," *IEEE Transactions on Industrial Electronics,* 2020.

[10] X. Ding, D. Zhang, J. Cheng, B. Wang, Y. Chai, Z. Zhao, R. Xiong, and P. C. K. Luk, "A Novel Active Equalization Topology for Series-Connected Lithium-ion Battery Packs," *IEEE Transactions on Industry Applications,* vol. 56, no. 6, pp. 6892-6903, 2020, doi: 10.1109/TIA.2020.3015820.

[11] A. C. Caliwag and W. Lim, "Hybrid VARMA and LSTM method for lithium-ion battery state-of-charge and output voltage forecasting in electric motorcycle applications," *IEEE Access,* vol. 7, pp. 59680-59689, 2019.

[12] Z. Wei, J. Zhao, C. Zou, T. M. Lim, and K. J. Tseng, "Comparative study of methods for integrated model identification and state of charge estimation of lithium-ion battery," *Journal of Power Sources,* vol. 402, pp. 189-197, 2018.

[13] H. Li, W. Zhang, X. Yang, H. Jiang, Y. Wang, T. Yang, L. Chen, and H. Shen, "State of charge estimation for lithium-ion battery using an electrochemical model based on electrical double layer effect," *Electrochimica Acta,* vol. 326, p. 134966, 2019.

[14] X. Shu, G. Li, Y. Zhang, S. Shen, Z. Chen, and Y. Liu, "Stage of Charge Estimation of Lithium-ion Battery Packs Based on Improved Cubature Kalman Filter with Long Short-Term Memory Model," *IEEE Trans. Transport. Electrific.,* pp. 1-1, 2020, doi: 10.1109/TTE.2020.3041757.

[15] Q. Song, Y. Mi, and W. Lai, "A novel variable forgetting factor recursive least square algorithm to improve the anti-interference ability of battery model parameters identification," *IEEE Access,* vol. 7, pp. 61548-61557, 2019.

[16] Z. Chen, X. Shu, R. Xiao, W. Yan, Y. Liu, and J. Shen, "Optimal charging strategy design for lithium‐ion batteries considering minimization of temperature rise and energy loss," *International Journal of Energy Research,* vol. 43, no. 9, pp. 4344-4358, 2019.

[17] K. S. Mawonou, A. Eddahech, D. Dumur, D. Beauvois, and E. Godoy, "Improved state of charge estimation for Li-ion batteries using fractional order extended Kalman filter," *Journal of Power Sources,* vol. 435, p. 226710, 2019.

[18] C. Chen, R. Xiong, R. Yang, W. Shen, and F. Sun, "State-of-charge estimation of lithium-ion battery using an improved neural network model and extended Kalman filter," *Journal of Cleaner Production,* vol. 234, pp. 1153-1164, 2019.

[19] S. Zhang, X. Guo, and X. Zhang, "An improved adaptive unscented kalman filtering for state of charge online estimation of lithium-ion battery," *Journal of Energy Storage,* vol. 32, p. 101980, 2020/12/01/ 2020, doi: https://doi.org/10.1016/j.est.2020.101980.

[20] J. Peng, J. Luo, H. He, and B. Lu, "An improved state of charge estimation method based on cubature Kalman filter for lithium-ion batteries," *Applied Energy,* vol. 253, p. 113520, 2019.

[21] X. Tang, Y. Wang, C. Zou, K. Yao, Y. Xia, and F. Gao, "A novel framework for Lithium-ion battery modeling considering uncertainties of temperature and aging," *Energ. Convers. Manage,* vol. 180, pp. 162-170, 2019.

[22] X. Shu, G. Li, J. Shen, W. Yan, Z. Chen, and Y. Liu, "An adaptive fusion estimation algorithm for state of charge of lithium-ion batteries considering wide operating temperature and degradation," *Journal of Power Sources,* vol. 462, p. 228132, 2020.

[23] Z. Xi, M. Dahmardeh, B. Xia, Y. Fu, and C. Mi, "Learning of battery model bias for effective state of charge estimation of lithium-ion batteries," *IEEE Transactions on Vehicular Technology,* vol. 68, no. 9, pp. 8613-8628, 2019.

[24] T. Mamo and F.-K. Wang, "Long Short-Term Memory with Attention Mechanism for State of Charge Estimation of Lithium-Ion Batteries," *IEEE Access,* 2020.

[25] R. Li, S. Xu, S. Li, Y. Zhou, K. Zhou, X. Liu, and J. Yao, "State of Charge Prediction Algorithm of Lithium-Ion Battery Based on PSO-SVR Cross Validation," *IEEE Access,* vol. 8, pp. 10234-10242, 2020.

[26] F. Yang, W. Li, C. Li, and Q. Miao, "State-of-charge estimation of lithium-ion batteries based on gated recurrent neural network," *Energy,* vol. 175, pp. 66-75, 2019.

[27] H. Chaoui and C. C. Ibe-Ekeocha, "State of charge and state of health estimation for lithium batteries using recurrent neural networks," *IEEE Transactions on vehicular technology,* vol. 66, no. 10, pp. 8773-8783, 2017.

[28] H. Zhang, W. Tang, W. Na, P.-Y. Lee, and J. Kim, "Implementation of generative adversarial network-CLS combined with bidirectional long short-term memory for lithium-ion battery state prediction," *Journal of Energy Storage,* vol. 31, p. 101489, 2020/10/01/ 2020, doi: https://doi.org/10.1016/j.est.2020.101489.

[29] E. Chemali, P. J. Kollmeyer, M. Preindl, R. Ahmed, and A. Emadi, "Long short-term memory networks for accurate state-of-charge estimation of Li-ion batteries," *IEEE Transactions on Industrial Electronics,* vol. 65, no. 8, pp. 6730-6739, 2017.

[30] X. Song, F. Yang, D. Wang, and K.-L. Tsui, "Combined CNN-LSTM network for state-of-charge estimation of lithium-ion batteries," *IEEE Access,* vol. 7, pp. 88894-88902, 2019.

[31] M. Fasahat and M. Manthouri, "State of charge estimation of lithium-ion batteries using hybrid autoencoder and Long Short Term Memory neural networks," *Journal of Power Sources,* vol. 469, p. 228375, 2020.

[32] Y. Tan and G. Zhao, "Transfer Learning With Long Short-Term Memory Network for State-of-Health Prediction of Lithium-Ion Batteries," *IEEE Transactions on Industrial Electronics,* vol. 67, no. 10, pp. 8723-8731, 2020, doi: 10.1109/TIE.2019.2946551.

[33] N. Guo, X. Zhang, Y. Zou, L. Guo, and G. Du, "Real-time predictive energy management of plug-in hybrid electric vehicles for coordination of fuel economy and battery degradation," *Energy,* vol. 214, p. 119070, 2021/01/01/ 2021, doi: https://doi.org/10.1016/j.energy.2020.119070.

[34] M. A. Hannan, M. H. Lipu, A. Hussain, and A. Mohamed, "A review of lithium-ion battery state of charge estimation and management system in electric vehicle applications: Challenges and recommendations," *Renewable and Sustainable Energy Reviews,* vol. 78, pp. 834-854, 2017.

[35] S. Zhang, X. Guo, and X. Zhang, "Multi-objective decision analysis for data-driven based estimation of battery states: A case study of remaining useful life estimation," *International Journal of Hydrogen Energy,* vol. 45, no. 27, pp. 14156-14173, 2020/05/18/ 2020, doi: https://doi.org/10.1016/j.ijhydene.2020.03.100.

[36] Y. Xing, W. He, M. Pecht, and K. L. Tsui, "State of charge estimation of lithium-ion batteries using the open-circuit voltage at various ambient temperatures," *Applied Energy,* vol. 113, pp. 106-115, 2014.